Phase-Separated Composite Films for Liquid Crystal Displays

Valery Vorflusev and Satyendra Kumar*

A method of preparing liquid crystal devices by phase separation of liquid crystal from its solution in a prepolymer, which results in adjacent layers of liquid crystal and polymer, is described. Liquid crystals in these phase-separated composite films exhibit electro-optical properties not observed in devices prepared by conventional methods, polymer dispersion, or polymer-stabilization methods. Devices incorporating ferroelectric liquid crystals have gray scale and switch 100 times faster at low fields than conventional surface-stabilized devices. This method makes it possible to prepare devices with liquid crystal film thickness comparable to optical wavelengths.

Electro-optical devices based on liquid crystals (LCs) have conventionally been prepared by sandwiching LCs between two glass substrates with alignment layers, typically rubbed polyimide, to facilitate alignment of the LC's optic axis in a predetermined configuration. An electric field is used to manipulate the cell birefringence and to create different optical states. In recent years, isotropic dispersions of microscopic LC droplets in polymer matrix have been developed (*1*–*4*). Polymer dispersed LC (PDLC) devices usually operate in the scattering mode, where the electric field is used not to change the birefringence but the extent of light scattered by LC droplets as a result of a mismatch of refractive indices at the droplet boundary. Here, we report a method of preparing LC-based electro-optic devices by anisotropic phase separation of LC from its solution in a prepolymer. This phase-separated composite film (PSCOF) method can, in general, be used to prepare multilayer structures—for example, perpendicular to substrates to form an electrically controllable optical grating. In the simplest case, it yields adjacent uniform layers of the LC and polymer. The configuration of the optic axis in the LC layer can be controlled with an alignment layer on the substrate closest to the LC layer. The operation of a PSCOF device relies on changes in its birefringence in response to an applied electric field, as in conventional displays.

The PSCOF technology has advantages in the ease of fabrication, mechanical ruggedness, high resistivity, and flexibility of fine tuning the optical path length without requiring spacers of precise thickness, but most importantly, PSCOF devices prepared with ferroelectric and antiferroelectric LCs reveal technologically desirable characteristics including gray scale in ferroelectric (FLC) and antiferroelectric (AFLC) LC cells and a new switching mode in AFLC devices. In FLCs, the domain wall switching is suppressed, and the switching times at low fields are found to be two orders of magnitude faster than the conventional surface-stabilized FLC (SSFLC) devices. With the PSCOF technology, it now appears possible to build commercial electro-optical devices with ferroelectric and antiferroelectric LCs.

The PSCOF method requires a pair of glass substrates coated with transparent electrodes of indium-tin oxide. One of the substrates is spin-coated with polyvinyl alcohol (PVA) and then rubbed for the LC alignment. They are separated by bead spacers of diameter d. A solution of the photocurable prepolymer NOA-65 and the LC, in the ratio 60:40, is introduced into the cell by capillary action at a temperature well above the isotropic-nematic phase transition. The phase separation is initiated by exposing the cell to ultraviolet (UV) light through the substrate without the PVA alignment layer. The source of UV light is a high-pressure mercury vapor lamp operated at 200 W for about 5 min. Phase separation results in a solidified film of polymer on the substrate close to the UV source and an LC film between the polymer film and the second substrate (Fig. 1). The LC (nematic, FLC, or AFLC) acquires a homogeneous alignment resulting from the influence of the alignment layer on the adjacent substrate. The LC and polymer films are uniform except in regions where the polymer-LC interface bonds to the opposite substrate (Fig. 2). These bonding sites are affected by the concentration and chemical nature of the LC compound, the alignment layer, the rate of phase separation, and the cell thickness d. The process can be optimized to reduce the average size and number of these bonding sites, resulting in an almost perfectly uniform LC film over the cell area (Fig. 2B), which we refer to as the PSCOF structure.

In PSCOF's incorporating an FLC, zigzag defects (*5*) are apparent under an optical microscope, confirming a continuous LC film. Measurements on PSCOF cells, prepared with different concentrations of nematic LC E7 and prepolymer NOA-65, show that the thickness of the LC layer depends on the amount of LC in the mixture and that only a small amount of LC is trapped in the polymer film. Light scattered by the trapped LC is found to be negligible.

The mechanism responsible for the formation of PSCOF is similar to anisotropic polymerization (*6*). Because the absorption of the UV light is predominantly by the LC molecules in the solution, an intensity gradient is produced in the sample. Consequently, NOA-65 molecules first undergo polymerization near the substrate closest to the UV source, and LC molecules are expelled from the polymerized volume, forcing them to move away from the source. Droplet formation is inhibited because of relatively slow rate of phase separation and fast diffusion of the relatively small LC molecules. Consequently, the phase-separated LC moves closer to the second substrate toward the region of lower UV intensity.

The presence of a PVA alignment layer on the substrate in contact with LC enhances the formation of uniform layers. In its presence, a PSCOF structure (parallel layer morphology) is obtainable at higher UV intensities (that is, faster phase separation) for the range (1 to 5 μm) of cell thicknesses that we have studied. This suggests that the LC material wets the PVA alignment layer and easily spreads over it. The LC molecules near the alignment layer respond to its anchoring potential and align parallel to the rubbing direction. The volume of aligned LC grows during the phase separation process. Oriented LC molecules determine the microscopic structure of the poly-

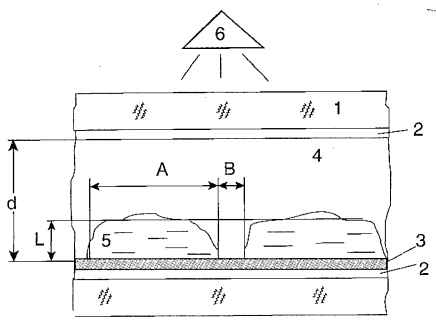

Fig. 1. Schematic of the internal structure of a PSCOF device. 1, glass substrates; 2, electrodes; 3, alignment layer; 4, solidified polymer; 5, liquid crystal; and 6, UV source. d is the cell thickness, which depends on the size of bead spacers used, and L and A are the average lateral and transverse dimensions of the LC volume. B dimension characterizes the areas where the polymer-LC interface binds to the substrate on the opposite side.

Department of Physics, Kent State University, Kent, OH 44242, USA.

*To whom correspondence should be addressed. E-mail: satyen@xray.kent.edu

mer-LC interface, which becomes compatible with their alignment. Although the use of one alignment layer can produce only homogeneously aligned cells, we have successfully prepared twisted nematic devices (*4*) by adding a chiral dopant.

The PSCOF technology provides a number of advantages. First, LC films of practically any thickness can be prepared without spacers of that size. This enables one to precisely fine tune the optical path length of the device. Devices with uniform and homogeneously aligned nematic LC film of thicknesses as small as 0.8 μm (~200 molecules) have been successfully prepared with 3-μm spacers. Still thinner films are possible. Second, the polymer bonds to the substrate adjacent to the LC at a large number of randomly distributed microscopic points, thus giving it rigidity and strength and thereby decreasing the sensitivity to external mechanical deformations without compromising performance. Such mechanical deformations can render the SSFLC devices (*7*) impractical and have been one of the major obstacles to their commercialization. Measurements on 5-cm-long plastic substrate cells, deformed in the middle by 1 cm to form an arc, reveal no internal changes in the director configuration. Under a high local pressure, such cells exhibit temporary changes in thickness. Their thickness reverts to the original value within 5 to 30 s after the pressure is released. PSCOF devices appear to be ideally suited for flexible displays. Third, only one alignment layer is required to align the LC. The results presented here are obtained on PSCOF cells with only one alignment layer. In active matrix devices, the substrate with thin-film-transistors (TFTs) can be selected to be the one without alignment layer, thus eliminating the need for mechanical rubbing, which damages the TFT array and reduces the yield. Fourth, the polymer film deposited on the TFT substrate increases the overall resistivity and thus the charge holding time to several seconds (for example, more than 3.5 s for FLC devices). Other advantages of PSCOFs lie in the modification of the electro-optical behavior of LC phases.

The SSFLC cells exhibit bistability (*7*) and electric field–dependent switching times (Fig. 3A). In a PSCOF device containing the LC Felix-15-100 (Hoechst, Germany), switching at low fields is two orders of magnitude faster than in SSFLC. Also, the switching angle, which is the difference in molecular orientations in the "on" and "off" states, is found to continuously depend on the applied field (Fig. 3B). The switching angle in an FLC device determines its optical transmission between cross-polarizers. Consequently, they have a continuous and natural gray scale that is necessary in most applications. Overall light throughput in PSCOFs is much higher than in ferroelectric PDLCs (PDFLCs) (*8*) because the light scattering from the small number of LC droplets embedded in the polymer film is much smaller than in PDFLC. The switching voltages are also much smaller than those of the PDFLC (Fig. 3B).

The electro-optical response of an AFLC-PSCOF is different from that of the pure AFLC behavior. In the latter, the antiferroelectric order is deformed at small field strengths and, at high fields, a sharp transition from the antiferroelectric to the field-induced ferroelectric state is observed (*9*). This behavior is illustrated in the dependence of the apparent switching angle on the applied voltage at 75°C in the antiferroelectric phase of the LC MHPOBC (Fig. 4). After the field has been switched off, the system returns to the same antiferroelectric state. In the PSCOF structure, AFLCs exhibit threshold-less response without a transition to the field-induced ferroelectric phase. AFLC order in PSCOFs is able to withstand much higher deformation and provide a gray scale. Furthermore, AFLCs exhibit optical memory (bistability). The optical transmission levels in the stable states in which these devices are left after applications of positive and negative pulses are different.

The mesogenic properties of LCs do not play any role in the formation of PSCOFs. The phase separation can be performed in the isotropic phase, which widens the range of

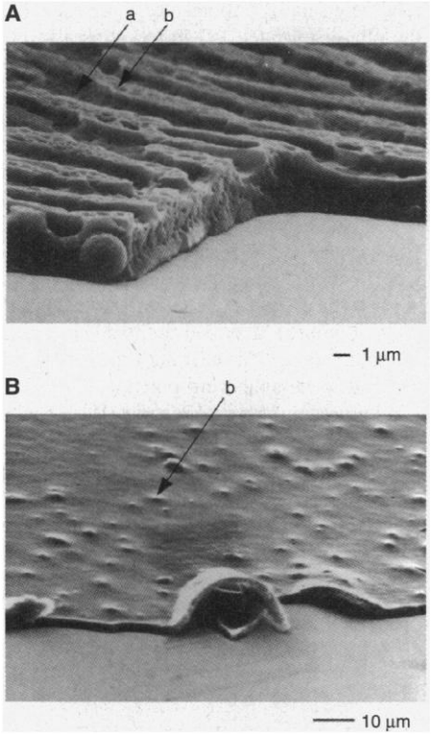

Fig. 2. Scanning electron micrographs of the polymer film structure taken after removing the substrate close to the LC and washing away the LC. The volume filled with LC (a) and the areas that were in contact with the opposite substrate (b) are indicated. (**A**) At 20% LC concentration, grooves or elongated LC droplets form along the rubbing direction after the phase separation. (**B**) The formation of nearly uniform parallel layers of LC and polymer (that is, a PSCOF structure) is confirmed for 40% LC at the same rate of phase separation as in (A). At a faster rate of phase separation, PDLCs are formed.

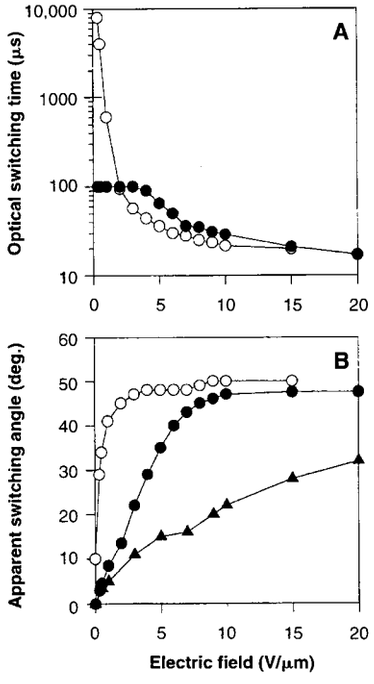

Fig. 3. Comparison of electro-optical properties of SSFLC (○), PSCOF (●), and PDFLC (▲) at room temperature in cells of 1.7, 3.0, and 5.0 μm, respectively. (**A**) Optical switching times and (**B**) apparent switching angle versus the amplitude of the square-wave electric field were measured with 40 wt % of the LC Felix-15-100 for PSCOF and 20 wt% for PDFLC.

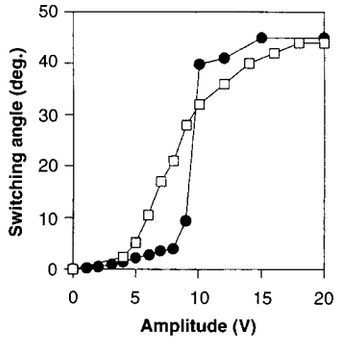

Fig. 4. Comparison of electro-optical response of the antiferroelectric phase of MHPOBC in SSFLC (●) and PSCOF (□) devices. At low field, antiferroelectric order is deformed followed by a transition to the ferroelectric state in SSFLC, whereas the AFLC order in PSCOFs can withstand much higher deformations exhibiting a gray scale.

possible applications of the PSCOF technology to nonliquid crystalline areas. This technology should permit one to prepare sandwiches of LCs between polymer films and vice versa and self-supporting thin and flexible displays. Fabrication of multilayer structures perpendicular to the substrate, for use in switchable gratings and other diffractive optics applications, is possible with the use of masks during phase separation. Electrically controllable LC microlenses, two-dimensional optical gratings, and other microstructures have been prepared with the PSCOF method.

References and Notes

1. P. S. Drzaic, Ed., *Liquid Crystal Dispersions* (World Scientific, Singapore, 1995).
2. G. Crawford and S. Zumer, Eds., *Liquid Crystals in Complex Geometries* (Taylor & Francis, London, 1996).
3. J. W. Doane, N. A. Vaz, B.-G. Wu, S. Zumer, *Appl. Phys. Lett.* **48**, 269 (1986).
4. L. Blinov and V. Chigrinov, *Electrooptical Effects in Liquid Crystals* (Springer-Verlag, New York, 1993).
5. N. A. Clark, T. Rieker, J. Maclennanl, *Ferroelectrics* **85**, 79 (1988).
6. V. Krongauz, E. Schmelzer, R. Yohannan, *Polymer* **32**, 1654 (1991).
7. N. A. Clark and S. T. Lagerwall, *Appl. Phys. Lett.* **36**, 899 (1980).
8. V. Vorflusev and S. Kumar, *Ferroelectrics* **213**, 117 (1998).
9. A. Fukuda, Y. Takanishi, T. Isozaki, K. Ishikawa, H. Takezoe, *J. Mater. Chem.* **4**, 997 (1994).

10. Supported in part by NSF Science and Technology Center ALCOM grant DMR-89-20147.

12 November 1998; accepted 5 February 1999

An Adiabatic Quantum Electron Pump

M. Switkes,[1] C. M. Marcus,[1]* K. Campman,[2] A. C. Gossard[2]

A quantum pumping mechanism that produces dc current or voltage in response to a cyclic deformation of the confining potential in an open quantum dot is reported. The voltage produced at zero current bias is sinusoidal in the phase difference between the two ac voltages deforming the potential and shows random fluctuations in amplitude and direction with small changes in external parameters such as magnetic field. The amplitude of the pumping response increases linearly with the frequency of the deformation. Dependencies of pumping on the strength of the deformations, temperature, and breaking of time-reversal symmetry were also investigated.

Over the past decade, research into the electrical transport properties of mesoscopic systems has provided insight into the quantum mechanics of interacting electrons, the link between quantum mechanics and classical chaos, and the decoherence responsible for the transition from quantum to classical physics (*1, 2*). Most of this research has focused on transport driven directly by an externally applied bias. We present measurements of an adiabatic quantum electron pump, exploring a class of transport in which the flow of electrons is driven by cyclic changes in the wave function of a mesoscopic system.

A deformation of the confining potential of a mesoscopic system that is slow compared with the relevant energy relaxation times changes the wave function of the system while maintaining an equilibrium distribution of electron energies. In systems connected to bulk electron reservoirs by open leads supporting one or more transverse quantum modes, the wave function extends into the leads and these adiabatic changes can transport charge to or from the reservoirs. A periodic deformation that depends on a single parameter cannot result in net transport; any charge that flows during the first half-period will flow back during the second. On the other hand, deformations that depend on two or more parameters changing in a cyclic fashion can break this symmetry and, in general, can provide net transport. This transport mechanism was originally described by Thouless (*3*) for isolated (or otherwise gapped) systems at zero temperature. The theory has been extended to open systems at finite temperature (*4–6*). Here, we present an experimental investigation of this phenomenon.

Before we characterize the adiabatic quantum pump in the present experiment, it is useful to recall other mechanisms that produce a dc response to an ac driving signal in coherent electronic systems. One mechanism relies on absorption of radiation to create a nonequilibrium distribution of electron energies, which leads to photon-assisted tunneling (*7*) in systems with asymmetric tunneling leads and a mesoscopic photovoltaic effect (*8*) in open systems. A second mechanism, the classical analog of the quantum pumping measured in this experiment, has been observed in single (*9*) and multiple (*10*) quantum dots in which transport is dominated by the Coulomb blockade (*2*). In this regime, the capacitive energy needed to add a single electron to the system is greater than the temperature and applied bias, blockading transport through the dot. Electrons can be added one by one by changing the potential of the isolated dot relative to the reservoirs. Each cycle begins by isolating the system from one electron reservoir—for example, by increasing the height of one tunneling barrier—while forcing one or more electrons to enter from the other reservoir by changing the potential in the system. The cycle is continued by reversing the configuration to isolate the system from the reservoir that supplied the electrons and forcing the extra electrons out into the other reservoir, yielding a net flow quantized in units of the electron charge times the frequency applied. This cycle requires two ac control voltages with a phase difference between them. The magnitude and direction of the pumping are determined by these voltages; there are no random fluctuations due to quantum effects. The control and quantization of current provided by the Coulomb blockade pump has motivated its development for use as a precision current standard [see, for example, (*11*)].

Adiabatic quantum pumping in open structures also requires two ac voltages and produces a response that is linear in the ac frequency. However, because the system is open to the reservoirs, Coulomb blockade is absent and the pumping response is not quantized. Quantum pumping is driven not by cyclic changes to barriers and potentials, but by shape changes in the confining potential or other parameters that affect the interference pattern of the coherent electrons in the device.

Many aspects of adiabatic quantum pumping can be understood in terms of the emissivity, dn/dX, which characterizes the number of electrons n entering or leaving the device in response to a small change in some parameter δX, such as a distortion of the confining potential (*12*). The change in the charge of the dot is thus $\delta Q = e\Sigma\delta X_i dn/dX_i$. Integrating along the closed path in the i-dimensional space of parameters X_i defined by the pumping cycle then yields the total charge pumped during each cycle (*6*). For the particular case of pumping with two parameters (for example, shape distortions at two locations on the dot), the line integral can be written as an integral over the surface enclosed by the path, $Q \propto \int_\alpha \xi dX_1 dX_2$ (*6*), where ξ depends on the emissivities at points in parameter space enclosed by the path. Because changes in external parameters rearrange the electron interference pattern in the device, emissivities fluctuate randomly as parameters are changed, similar to the well-known mesoscopic fluctuations of conductance in coherent samples.

[1]Department of Physics, Stanford University, Stanford, CA 94305, USA. [2]Materials Department, University of California, Santa Barbara, CA 93106, USA.

*To whom correspondence should be addressed. E-mail: cmarcus@stanford.edu